

Crystal Structures and Curie's Temperature of ABO_3 Perovskite Ceramics with Different Ionic Radius

Jassim M. Yaseen

Department of physics, College of Education, Al-Iraqia University, Baghdad, IRAQ

Abstract

Barium titanate (BaTiO_3) is one of the most ferroelectrics. It's commonly used in capacitors due to its high dielectric constant. In this study, our goal is to determine the extent to which the change in the average ionic radius of A, B sites affects the structural, dielectric properties of this ceramic. In this study, barium titanate ($\text{Ba}_{0.85}\text{X}_{0.15}\text{TiO}_3$, $\text{BaY}_{0.15}\text{Ti}_{0.85}\text{O}_3$) ($\text{X} = \text{Pb, Ca, Co, Y} = \text{Zr, Si, Mn}$) was prepared by solid state reaction method in which the calcination temperature was 1200°C for 2 hours. Structural characterization and dielectric properties were determined and calculated by using x-ray diffractometer, RCL-Meter (PM6303) at frequency 20 Hz using different temperature respectively. The results of the work showed that the average ionic radius at the A, B sites plays a large and clear role in determining the values of the dielectric constant and Curie temperature in perovskites in addition to the structural parameters.

Keywords: Ceramic; Crystal structure; Perovskite; Crystallographic structure

Received: 10 October 2021; **Revised:** 24 January 2022; **Accepted:** 31 January; **Published:** 1 April 2022

1. Introduction

Barium titanate (BaTiO_3) is one of the most common ferroelectrics. Ferroelectricity is the spontaneous polarization in the absence of an electric field. The spontaneous polarization is a consequence of the positioning of the Ba^{+2} , Ti^{+4} and O^{2-} within the unit cell as in Fig. (1).

Under the ferroelectric curie temperature ($120\text{-}130^\circ\text{C}$), the unit cell of BaTiO_3 is tetragonal in which spontaneous polarization occurs as the titanium ions are displaced along the c-axis, but when BaTiO_3 is heated above this temperature, the unit cell became cubic (nonpolar phase) [3-5]. BaTiO_3 has a perovskite structure ($\text{A}^{+2}\text{B}^{+4}\text{O}_3$) in which ($\text{A} = \text{Ba}^{+2}$, $\text{B} = \text{Ti}^{+4}$). In this structure, Ba^{+2} coordinated by twelve oxygen ions, Ti^{+4} coordinated by 6 oxygen ions which form an octahedron as the structure in Fig. (1) [6]. This structure shows a cubic unit cell with large cation A on the corner, a smaller cation B in the body centers of the faces. BaTiO_3 was candidate for piezoelectric transducer applications and the ferroelectric multilayer ceramic capacitors (MLCCs) extremely important and widely used in many applications include capacitor, phonograph pickups, band pass filters, medical ultrasound, random access memories (RAMs), biocompatible, nanogenerators, etc. [7-9]. There are many studies that dealt with the preparation and study of BaTiO_3 . Sareecha et al. [10] have studied the temperature dependence of dielectric constant for pure and Pb-doped BaTiO_3 ceramics. Shuvo et al. [11] have found that doping BaTiO_3 with 20% PbO leads to develop dielectric properties [11]. Zhang et al. [12] have elaborated the internal mechanism for high piezoelectric response of $\text{Ba}(\text{Ti}_{0.8}\text{Zr}_{0.2})\text{O}_3$ - $(\text{Ba}_{0.7}\text{Ca}_{0.3})\text{TiO}_3$. Kim and Song [13] have found that addition of MgO (0.2-1 wt.%) leads to increase the dielectric permittivity while it decreases with addition of Y_2O_3 (0.3-1.5 wt.%). Butee et al. [14] have prepared the $\text{Ba}_{1-x}\text{Pb}_x\text{TiO}_3$ and found that the Curie's temperature increases from 120 to 180°C for $x=0.15$. Kadira et al. [15] have studied the effect of Ca^{+2} ion ($x=0.01\text{-}0.1$) on ferroelectric properties of $\text{Ba}_{1-x}\text{Ca}_x\text{TiO}_3$ and they found that the maximum Curie's temperature is at $x=0.05$. Islam et al. [16] have studied the effect of Mn^{+4} ions on the dielectric, microstructural properties of $\text{BaMn}_x\text{Ti}_{1-x}\text{O}_3$ ($x=0.0\text{-}0.04$).

The aim of this work is to indicate and verify that whether the radius of the ion added to the base ion in the (A-site= Ba^{+2}) and (B-site= Ti^{+4}). In other words, the average ionic radius has an effect on

ferroelectric Curie's temperature. Note that there are articles have shown that the ionic radius $\langle r_{A\text{-site}} \rangle$ of A-site ions affects strongly the Curie's temperature [17].

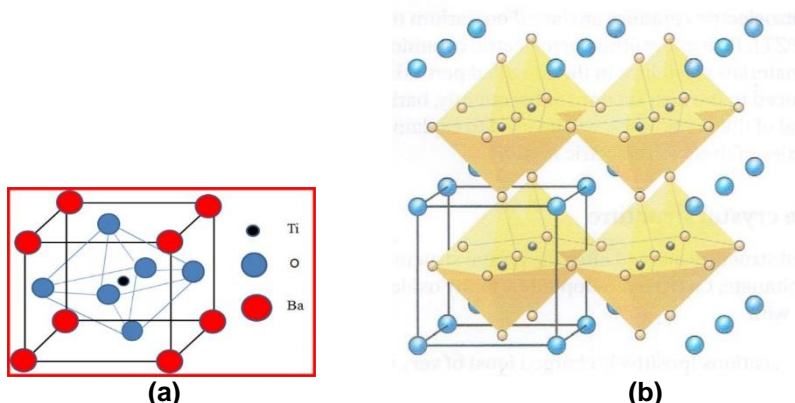


Fig. (1) (a) Structure of perovskite ABO_3 unit cell structure of $BaTiO_3$, (b) Perovskite structure as connected network of octahedral

2. Experimental Part

After performing the processes of weighing the used compounds according to the proportions mentioned in table (2), in which the mole ratio for both $BaCO_3$ and TiO_2 used in this work was [1:1] according to [18,19].

Table (1) Chemical compounds used in this work

No.	Compound	Origin	Purity (%)	Impurities (%)
1	TiO_2	BDH Chemicals Ltd (England)	98	Fe (0.5) L.I (0.5)
2	ZrO_2		98	HCl (0.005) Fe (0.002)
3	PbO (analar)		99	
4	CoO (black)			
5	$BaCO_3$	Riedel-De Haen (Germany)	99	Ca (0.01) Fe (0.001) Cl (0.005) NO_3 (0.005)
6	MnO_2		95	
7	SiO_2		99.51	
8	$CaCO_3$	Panreac Quimica SA (Spain)		

The wet mixing process was performed by using magnetic stirrer with heating at 70 °C after adding distilled water to the beakers containing prepared powders for a better reaction process. The mixing process lasted for 1 hour. After that, these beakers were placed in the oven at 150 °C for 2 hours to dry the samples. Then, these samples were grinded using a gate mortar for more homogeneity, and to check the prepared phase, samples were examined by the x-ray diffraction (XRD) technique using Philips PW 1316/90, single pen recorder ($Cu K\alpha$ Target). After that, the samples were calcined in a muffle furnace at 1200 °C for 2 hours at heating rate of 8 °C/min. The calcined samples were strongly grinded using ball milled process to get the smallest grain size. The samples were placed in a cylindrical container with two stainless steel balls in which the crushing process holder is performed after placing the container on a vibrating stand for 2 hours.

Then, the crushed samples were pressed using hydraulic press as discs with diameter of 2 cm and thickness of 3-5 mm as shown in Fig. (2). For a coherent and regular shape, the PVA binder was used. The discs were sintering at 1200 °C for 2 hours at heating rate of 6 °C/min after remaining at 500 °C for 30 minutes to expel the binder and to prevent the cracks that led to damage the discs.



Fig. (2) Discs of prepared samples with 3-5mm thickness and 20mm diameter (in muffle furnace)

The grain size of samples were calculated depending on the XRD patterns using Scherrer's equation:

$$D = \frac{K \lambda}{\beta \cos \theta} \quad (1)$$

where D is mean crystallite size, K is Scherrer's constant, λ is diffraction wavelength, and β is the full-width at half-maximum (FWHM)

To calculate the dielectric constant versus temperature, determination of Curie's temperature from the Eq. (2) was used after measuring the electrical capacitance of the samples by using RCL-Meter (PM6303) at frequency of 20 Hz and electrical oven as a source of temperature.

$$\epsilon_r = \frac{C d}{\epsilon A} \quad (2)$$

here, C , d , A and ϵ represent the capacitance, thickness of samples, surface area of capacitors, and space permittivity (8.85×10^{-12} F/m), respectively

3. Results and Discussion

Figures (3) to (9) show the XRD patterns of BaTiO_3 , $\text{Ba}_{0.85}\text{Pb}_{0.15}\text{TiO}_3$, $\text{Ba}_{0.85}\text{Ca}_{0.15}\text{TiO}_3$, $\text{Ba}_{0.85}\text{Co}_{0.15}\text{TiO}_3$, $\text{BaZr}_{0.15}\text{Ti}_{0.85}\text{O}_3$, $\text{BaSi}_{0.15}\text{Ti}_{0.85}\text{O}_3$, $\text{BaMn}_{0.15}\text{Ti}_{0.85}\text{O}_3$, respectively. Figure (3) shows the good growth of the BaTiO_3 phase with the appropriate intensity of the main characteristic peaks of this phase namely [100], [101], [111], [002], [200], [201], [211], [202], [220], [301], [310] at $2\theta=22.317^\circ$, 31.705° , 39.060° , 45.150° , 45.510° , 50.820° , 56.356° , 65.960° , 66.242° , 74.620° , and 75.230° . In addition, no impurities were found in this phase and the calcination at 1200°C for 2 hours is appropriate to prepare BaTiO_3 phase in BaO-TiO_2 by using solid state reaction method.

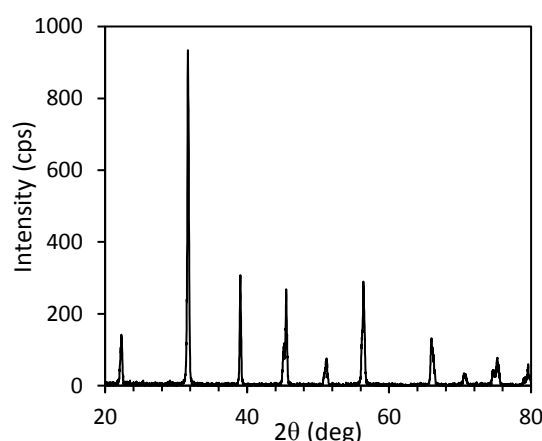


Fig. (3) XRD pattern of BaTiO_3 ceramic calcined at 1200°C for 2 hrs

Figures (4) and (5) also show good growth of the $\text{Ba}_{0.85}\text{Pb}_{0.15}\text{TiO}_3$ and $\text{Ba}_{0.85}\text{Co}_{0.15}\text{TiO}_3$ phases with no observed characteristic impurities except of the small intensity peak at $2\theta=29.170^\circ$ that belongs to PbO compound in Fig. (2). In Fig. (6), two peaks can be observed with distinguished intensities as they belong to CaO compound. This indicates the need to raise the calcination temperature to more than 1200°C , and the evidence is that the phase growth has not been healed as required.

Figures (7), (8) and (9) also show good growth of $\text{BaZr}_{0.15}\text{Ti}_{0.85}\text{O}_3$, $\text{BaMn}_{0.15}\text{Ti}_{0.85}\text{O}_3$ and $\text{BaSi}_{0.15}\text{Ti}_{0.85}\text{O}_3$, respectively, with no observed characteristic impurities except in Fig. (5) at $2\theta = 28.830^\circ$ that belongs to ZrO_2 (JCPDS, 42-1164), and in Fig. (6) at $2\theta = 26.350^\circ$ that belongs to MnO_2 , and in Fig. (7) at $2\theta = 29.020^\circ$ that belongs to SiO_2 (JCPDS, 40-1498).

Tables (2) and (3) show the crystal dimensions (a , c , c/a) and average crystallite size of prepared groups. By looking at tables (2) and (4), it can be found that the ratio c/a increases with decreasing average ionic radius of the site A in the structure of perovskites ABO_3 except for the group (4) where it remains relatively constant. As for the B site, there is no fixed relationship was found between the average ionic radius and the value of a , while the c/a ratio is greatly affected by the average ionic radius, as it increases with its increase and decreases with its decrease.

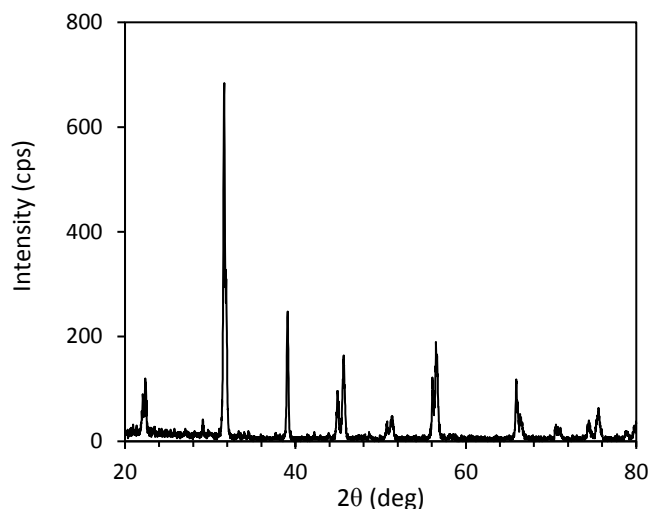


Fig. (4) XRD pattern of $\text{Ba}_{0.85}\text{Pb}_{0.15}\text{TiO}_3$ ceramic calcined at 1200°C for 2 hrs

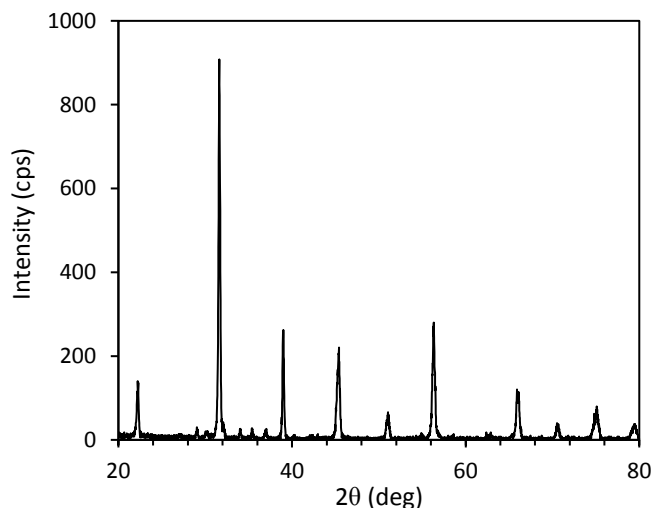


Fig. (5) XRD pattern of $\text{Ba}_{0.85}\text{Co}_{0.15}\text{TiO}_3$ ceramic calcined at 1200°C for 2 hrs

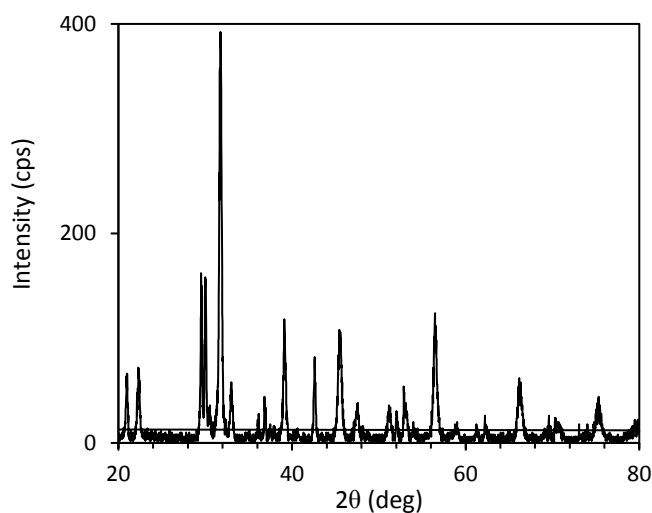


Fig. (6) XRD pattern of $\text{Ba}_{0.85}\text{Ca}_{0.15}\text{TiO}_3$ ceramic calcined at 1200°C for 2 hrs

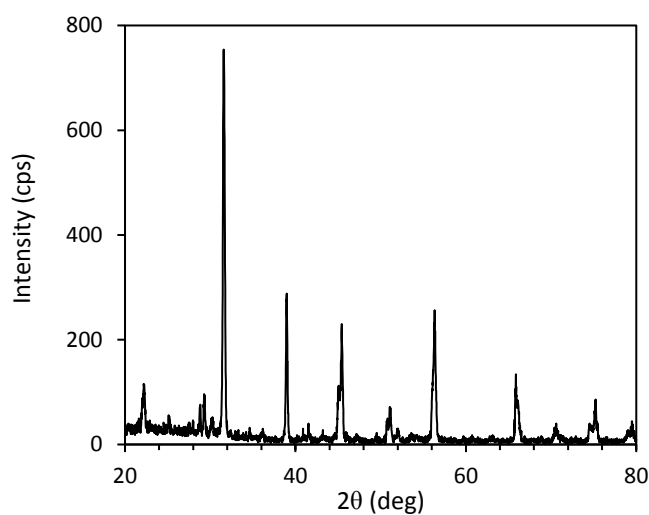


Fig. (7) XRD pattern of $\text{BaZr}_{0.15}\text{Ti}_{0.85}\text{O}_3$ ceramic calcined at 1200°C for 2 hrs

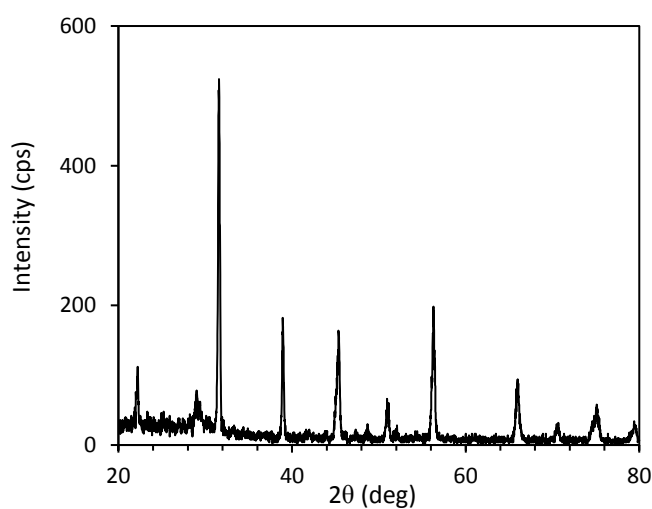


Fig. (8) XRD pattern of $\text{BaSi}_{0.15}\text{Ti}_{0.85}\text{O}_3$ ceramic calcined at 1200°C for 2 hrs

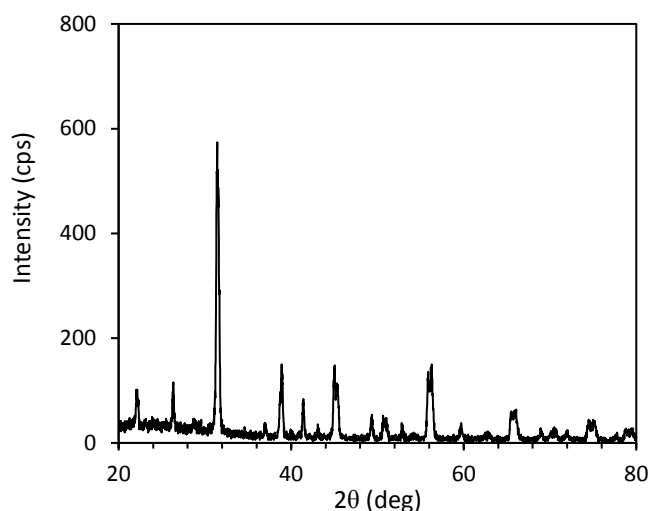


Fig. (9) XRD pattern of $\text{BaMn}_{0.15}\text{Ti}_{0.85}\text{O}_3$ ceramic calcined at 1200°C for 2 hrs

Figure (10) shows that the dielectric constant increases with increasing temperature at different rates from room temperature to temperatures close to Curie's temperature. This behavior is similar for all the prepared groups except for the group $\text{Ba}_{0.85}\text{Co}_{0.15}\text{TiO}_3$, where it is clearly seen that it is more stable in its dielectric constant within the thermal range 60-90 °C. Also, it is note that upon reviewing the radii of the ions that were compensated at the two sites A and B in the composition of perovskites ABO_3 (table 2).

It was found that the decrease in the average ionic radius leads to a clear and large decrease in the dielectric constant at Curie's temperature, while increasing the average of the ionic radius at the site B leads to an increase in the value of the dielectric constant at Curie's temperature, as in the case when the relative substitution of Zr^{+4} ion instead of Ti^{+4} in the $\text{BaZr}_{0.15}\text{Ti}_{0.85}\text{O}_3$ group. Although, this cannot be generalized in absolute terms only after many appropriate experiments. The effect of the difference in the ionic radius for example between Zr^{+4} and Ti^{+4} ions in $\text{BaZr}_{0.15}\text{Ti}_{0.85}\text{O}_3$ group lead to octahedral oxygen distortion. This can be generalized to the rest of the prepared groups and it is believe that this may have the largest role in changing the values of the dielectric constant and Curie's point.

Table (2) The crystal dimensions of groups

No.	Material	a (Å)	c (Å)	c/a
1	BaTiO_3	3.982	4.012	1.0075
2	$\text{Ba}_{0.85}\text{Pb}_{0.15}\text{TiO}_3$	3.980	4.030	1.0125
3	$\text{Ba}_{0.85}\text{Ca}_{0.15}\text{TiO}_3$	3.971	4.023	1.0131
4	$\text{Ba}_{0.85}\text{Co}_{0.15}\text{TiO}_3$	3.980	4.009	1.0073
5	$\text{BaZr}_{0.15}\text{Ti}_{0.85}\text{O}_3$	3.996	4.028	1.0080
6	$\text{BaSi}_{0.15}\text{Ti}_{0.85}\text{O}_3$	3.996	4.006	1.0025
7	$\text{BaMn}_{0.15}\text{Ti}_{0.85}\text{O}_3$	3.995	4.013	1.0045

Table (3) Crystallite size of prepared groups

No.	Material	Crystallite size (nm)	Average crystallite size (nm)
1	BaTiO_3	252 - 335	293.5
2	$\text{Ba}_{0.85}\text{Pb}_{0.15}\text{TiO}_3$	388 - 407	397.5
3	$\text{Ba}_{0.85}\text{Ca}_{0.15}\text{TiO}_3$	234.91 - 266.5	250.70
4	$\text{Ba}_{0.85}\text{Co}_{0.15}\text{TiO}_3$	330 - 396	363
5	$\text{BaZr}_{0.15}\text{Ti}_{0.85}\text{O}_3$	356 - 374	365
6	$\text{BaSi}_{0.15}\text{Ti}_{0.85}\text{O}_3$	330 - 388.04	359.02
7	$\text{BaMn}_{0.15}\text{Ti}_{0.85}\text{O}_3$	213.23 - 374.6	293.915

Table (4) The groups prepared in this work

No.	Compositions	$\langle r_{A\text{-site}} \rangle$	$\langle r_{B\text{-site}} \rangle$
1	BaTiO ₃	1.61	0.605
2	Ba _{0.85} Pb _{0.15} TiO ₃	1.592	
3	Ba _{0.85} Ca _{0.15} TiO ₃	1.569	
4	Ba _{0.85} Co _{0.15} TiO ₃	1.480	
5	BaZr _{0.15} Ti _{0.85} O ₃		0.622
6	BaSi _{0.15} Ti _{0.85} O ₃		0.574
7	BaMn _{0.15} Ti _{0.85} O ₃		0.593

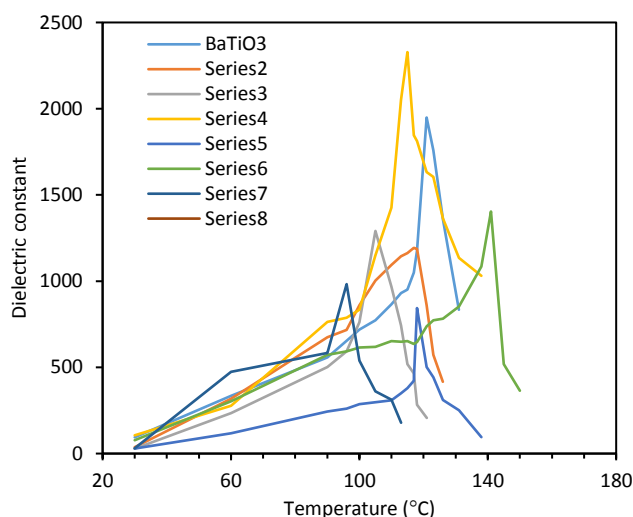


Fig. (10) Dielectric constant of prepared groups vs. temperature at 20 Hz, Series 2: BaMn_{0.15}Ti_{0.85}O₃, Series 3: BaSi_{0.15}Ti_{0.85}O₃, Series 4: BaZr_{0.15}Ti_{0.85}O₃, Series 5: Ba_{0.85}Ca_{0.15}TiO₃, Series 6: Ba_{0.85}Pb_{0.15}TiO₃, Series 7: Ba_{0.85}Co_{0.15}TiO₃

4. Conclusions

In concluding remarks, the temperature of 120 °C for 2 hours is suitable for preparing BaTiO₃. The effect of the average ionic radius on the displacement rate of the main peaks of the prepared compound can be observed. The occurrence of a creep and a shift in the direction of the decrease in the 2θ value of the main peaks, especially when the value of the average ionic radius changes in the B-site where we find the large relative displacement of the (110) peak of the groups (BaZr_{0.15}Ti_{0.85}O₃, BaSi_{0.15}Ti_{0.85}O₃, BaMn_{0.15}Ti_{0.85}O₃). To develop a comprehensive general relationship linking the average ionic radius at the A,B sites in the composition of perovskites and between the crystal structure, its dimensions and the granular size, we must discuss and take into account other factors related to the physical and structural properties of the ion or the added oxide, the most important of which is the melting point. The average ionic radius at the A,B sites plays a large and clear role in determining the values of the dielectric constant and Curie temperature in perovskites.

References

- [1] J.C. Burfoot, "Ferroelectrics, An Introduction to The Physical Principles", D. van Nostrand Co. Ltd. (1967).
- [2] M. Singh et al., "Synthesis and Characterization of Perovskite Barium Titanate Thin film and its Application as LPG sensor", J. Sen. Actuat., (2017) 1170-1178.
- [3] K. Uchino, "Ferroelectric Devices", 2nd ed., CRC Press, Taylor & Francis Group (2009).
- [4] M.B. Smith et al., "Crystal Structure and The Paraelectric-to-Ferroelectric Phase Transition of Nanoscale BaTiO₃", J. Am. Chem. Soc., (2008) 6956-6963.
- [5] P. Groen and J. Holterman, "An Introduction to Piezoelectric Materials and Applications", Stichting Applied Piezo, Netherlands (2013).
- [6] P. Groen and J. Holterman, "An Introduction to Piezoelectric Materials and Applications", Stichting Applied Piezo, Netherlands (2012).
- [7] K.R. Kambale, A.R. Kulkarni and N. Venkataramani, "Synthesis of Barium Titanate Powder Using Nanosized Titania", Int. J. Innov. Res. Sci. Eng. Technol., 3(6) (2014).
- [8] S. Riaz et al., "Barium titanate films for electronic applications: structural and dielectric properties", Surf. Rev. Lett., 15(3) (2008) 237-244.
- [9] M. Acosta et al., "BaTiO₃-based piezoelectrics: Fundamentals, current status, and perspectives", Appl. Phys. Rev., 4 (2017).

- [10] N. Sareecha et al., "Fabrication and electrical investigations of Pb-doped BaTiO₃ ceramics", *Mater. Chem. Phys.* 193 (2017) 42-49.
 - [11] S.N. Shuvo, S. Saha and M. Rahman, "Dielectric and microstructural properties of PbO doped BaTiO₃", *Int. J. Innov. Sci. Mod. Eng.*, 3(8) (2015).
 - [12] Y. Zhang, H. Sun and W. Chen, "A brief review of Ba(Ti_{0.8}Zr_{0.2})O₃-(Ba_{0.7}Ca_{0.3})TiO₃ based lead-free piezoelectric ceramics: past, present and future perspectives", *J. Phys. Chem. Solids*, 114 (2018) 207-219.
 - [13] H.D. Kim and J.T. Song, "The dielectric and electrical properties of a X7R multilayer ceramic capacitor", *J. Cer. Process. Res.*, 12(3) (2011) 322-326.
 - [14] S. Butee et al., "Significant improvement in curie temperature and piezoelectric properties of BaTiO₃ with minimum Pb addition", *J. Asian Ceram. Soc.*, 7(4) (2019) 407-416.
 - [15] L. Kadir, A. Elmesbahi and S. Sayouri, "Dielectric study of calcium doped barium titanate Ba_{1-x}Ca_xTiO₃ ceramics", *Int. J. Phys. Sci.*, 11(6) (2016) 71-79.
 - [16] S. Islam et al., "Structural, dielectric and electric properties of manganese-doped barium titanate", *Int. J. Nanoelectro. Mater.*, 11(4) (2018) 419-426.
 - [17] A. Berenov, F. Le Goupil and N. Alford, "Effect of ionic radii on the curie temperature in Ba_{1-x-y}Sr_xCa_yTiO₃ compounds", *Sci. Rep.*, DOI:10.1038/srep28055 (2016).
 - [18] X. Liu et al., "Phase equilibria and thermodynamic evaluation of BaO-TiO₂-YO_{1.5} system", *J. Euro. Ceram. Soc.*, 38 (2018) 5430-5441.
 - [19] S. Lee and C. Randall, "Modified phase diagram oxide -titanium dioxide system for the ferroelectric barium titanate", *J. Am. Ceram. Soc.*, 90(8) (2007) 2589-2594.
 - [20] A. Elbasset et al., "Influence of Zr on structure and dielectric behavior of BaTiO₃ ceramics", *Indian J. Sci. Technol.*, 8(13) (2015). doi: thi0.17485/ijst/2015
-